Materials Advances

ROYAL SOCIETY OF CHEMISTRY

REVIEW

View Article Online
View Journal | View Issue

Cite this: *Mater. Adv.*, 2024, **5**, 4958

The past, present, and future of *in vivo*-implantable recording microelectrodes: the neural interfaces

Kun Liu,†[a] Hao Zhang,†[a] Minghui Hu,[b] Zifa Li,[b] Kaiyong Xu,[b] Dan Chen,[b] Wenqiang Cui,[c] Cui Lv,[d] Ran Ding,*[e] Xiwen Geng*[a] and Sheng Wei *[a]

The electrical signals between neurons are crucial in human perception, emotions, and behaviors. Abnormal activities of these signals are associated with sensory organ disorders such as pain, visual and auditory impairments, and neurological disorders including depression, paralysis, and epilepsy. The use of implanted microelectrodes for detecting and intervening in neuronal activity plays a significant role in diagnosing and treating diseases. Notably, as a key component of brain–computer interfaces (BCI), the rapid advancement of BCI technology has expanded the application of implantable recording microelectrodes in treating brain dysfunction. The transition from metal to flexible electrodes has marked significant advancements in materials and properties (biocompatibility, resolution and number of sites, stability, and functional integration, *etc.*) as well as surface modifications. However, these advancements also present challenges and shortcomings, particularly regarding the biocompatibility and electrochemical properties of electrodes. This paper reviews the development history of electrodes and common types, addressing the biocompatibility and electrochemical performance issues and their advances and future development directions. This discussion aims to serve as a reference for further improvements in electrode performance.

Received 11th December 2023,
Accepted 7th May 2024

DOI: 10.1039/d3ma01105d

rsc.li/materials-advances

1. Introduction

The human brain comprises hundreds of billions of neurons connected through millions of synapses. The electrical signals between neurons serve as a crucial pathway for information transmission, significantly impacting human cognition and behaviour. Electrode implantation can treat neurological diseases such as depression[1] and epilepsy[2] as well as neurodegenerative diseases like Parkinson's disease[3] and sensory organ abnormalities.[4] Neural recording microelectrodes are vital in diagnosing and treating neuropsychiatric disorders.

According to the degree of invasion, neural recording electrodes can be divided into non-invasive, semi-invasive, and invasive electrodes[5] (Fig. 1A). Specifically, non-invasive electrodes can record brain information through head-wearing devices that do not cause any skull or brain injury. These methods have low signal acquisition speeds and are only used for cursory recording, because they are affected by multiple sources of interference, such as the skull, scalp, cerebrospinal fluid, and

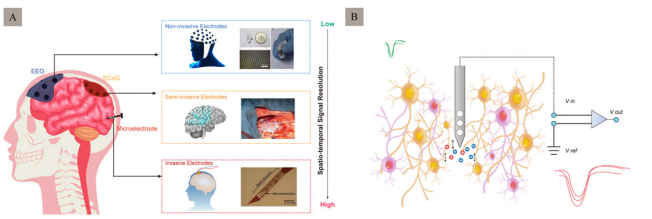

Fig. 1 Schematic diagrams and examples of three representative electrodes and principles of extracellular recording with implantable recording electrodes. (A) Schematic diagrams and examples of representative electrodes for three levels of invasion are shown (EEG, ECoG, and microelectrode recorded signals, with increasing resolution in that order. Each of the three example diagrams is reproduced with permission from ref. 12–14). (B) Principles of extracellular recording with implantable neural recording electrodes.

[a] *Key Laboratory of Traditional Chinese Medicine Classical Theory, Ministry of Education, Shandong University of Traditional Chinese Medicine, Ji'nan, 250355, P. R. China. E-mail: weisheng@sdutcm.edu.cn, xwgeng@sdutcm.edu.cn*
[b] *Chinese Medicine and Brain Science Interdisciplinary Research Center, Shandong University of Traditional Chinese Medicine, Ji'nan, 250355, P. R. China*
[c] *First College of Clinical Medicine, Shandong University of Traditional Chinese Medicine, Ji'nan, 250000, P. R. China*
[d] *Laboratory of Immunology for Environment and Health, Shandong Analysis and Test Centre, School of Pharmaceutical Sciences, Qilu University of Technology (Shandong Academy of Sciences), Ji'nan, 250355, P. R. China*
[e] *Institute for Translational Neuroscience, Second Affiliated Hospital of Nantong University, Nantong, 226000, P. R. China. E-mail: randing@ntu.edu.cn*
† These authors contributed equally to this work and share the first authorship.

strong tissue filtering, which can reduce the spatial resolution and information content of the signal. Electroencephalography (EEG)[6] is a typical non-invasive recording mode that can acquire signals by recording the amplified signal of spontaneous excitation potentials in the brain from the scalp. In contrast to non-invasive methods, invasive but non-penetrating electrodes that record information from the intracranial cortex are placed under the skull and on the cortex, to directly record neural signals from the cortical surface,[7] such as the electrocorticogram (ECoG).[8] Compared to non-invasive electrodes, these are faster to acquire and provide a more long-term stable signal. These penetrate deep into the brain parenchyma, achieve signal recording through intracortical recording interfaces, and record low-pass filter brain signals.[9] Their main function is to record and transmit micro- to millivolt-scale signals from small, localised neuronal populations in the brain which are generally used for short-term acute signal recording in patients requiring brain surgery[10] (*e.g.*, epilepsy focal resection surgery).

Implanted in the cerebral cortex or deep nucleus, invasive neural recording electrodes position the electrode tips close to or even within neurons.[11] This approach causes more tissue damage but achieves higher spatial resolution and a better signal-to-noise ratio (SNR) than non-invasive methods. It holds greater clinical application value and prospects. Implantable neural recording electrodes can be used to record electrical neural signals in two main ways: intracellular and extracellular. Compared with intracellular recording, electrodes for extracellular recording (Fig. 1B) can be inserted around the target neuron, and do not necessarily penetrate the cell membrane, which can keep cell function intact, record real neuronal electrical activity, and enable longer recording times. Therefore, it is the most used method for detecting neuronal activity in awake and free-moving objects.

2. Comment types and advances of implantable neural recording electrodes

Neural recording electrodes have evolved significantly since Galvani's discovery of bioelectricity in 1791, enriching neuroelectrophysiology theory and advancing related technology. In 1929, Berger first recorded EEG signals in humans. In 1939, Hodgkin and Huxley used microelectrodes to record action potentials (AP) from within neurons for the first time using the giant axons of squid. Michigan electrodes were introduced in 1970,[15] and in 1973, Vidal proposed the concept of brain–computer interfaces. Entering the 21st century, electrodes have seen rapid development not only in material optimization but also in performance, aiming at biocompatibility, high density, and multifunctionality. Fig. 2 illustrates the main advances in neural recording electrodes. This section introduces the main types of electrodes and the latest advances in electrode development.

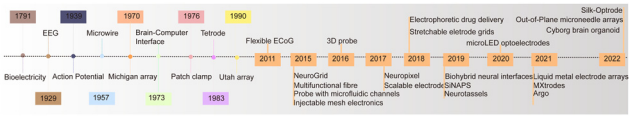

Fig. 2 Major developments in neural recording electrodes.

2.1 Microwire electrode and microelectrode arrays

The first implantable electrodes to enable long-term recordings in the brain were developed in the 1950s and were made of tungsten wire, a microwire electrode that was insulated except for at the tip.[16]

Metal microwire electrodes are generally made of stainless steel,[17] tungsten, gold, platinum, iridium, and other metals and alloys of these metals,[18] which exhibit good corrosion resistance and are simple. Commercial metal wires with diameters of 20–50 μm are usually used as production materials. The outer surface is wrapped with a thin insulating layer, and the end forms a bare plane or conical tip. When these bare surfaces touch the surfaces of neurons, their firing activities can be recorded. They are generally used to record APs or local field potentials (LFP) signals of neurons in animal brains. Microwire electrodes have different designs, such as single-wire, tetrode,[19] and multi-wire electrodes[20] (Fig. 3A–C). In 2003, Nicolelis *et al.*[21] implanted multiple 128-channel wire microelectrodes into the brains of adult macaques and recorded neuronal signals for up to 18 months, while recording 247 neurons (Fig. 3D).

Although microwire electrodes are straightforward to prepare, stable, inexpensive, and commonly utilized for deep brain stimulation, they face limitations in physical properties such as Young's modulus and bending stiffness. The bending stiffness

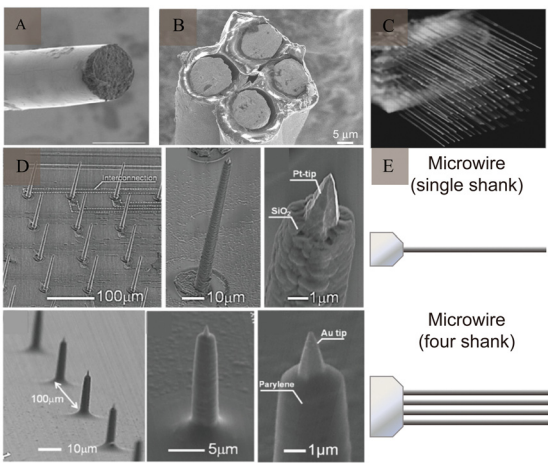

Fig. 3 Example of microwire and microelectrode arrays. (A) SEM image of a fabricated soft wire tip. Reproduced with permission from ref. 24. (B) SEM image of a tetrode. Reproduced with permission from ref. 25. (C) SEM image of a multi-wire electrode. Reproduced with permission from ref. 21. Copyright (2003) National Academy of Sciences, U.S.A. (D) SEM images of the fabricated nanotip microwire arrays. Reproduced with permission from ref. 23. (E) Schematic diagram of the generation design of microwires (adapted from ref. 26). SEM, scanning electron microscopy.

of metal microwires ranges between 10^{-4} and 10^{-3} N m. Flexible microwire electrodes lack sufficient rigidity and may bend during implantation, reducing the accuracy of the target site. To address this issue, some studies have suggested that auxiliary devices can facilitate accurate placement. In addition, the consistency of electrode performance cannot be guaranteed, because they are mainly prepared by means of manual integration. After implantation, microelectrodes are anchored through the skull into the tissue, leading to potential relative movement between the electrodes and the skull, as well as between the electrodes and brain tissue. This decreases the accuracy of the position and aggravates the rejection reaction of the brain tissue, leading to problems such as compression of the bottom tissue, failure of the insulation material, and spalling/corrosion of the metals. Furthermore, microwires have high impedance and are susceptible to motion artifacts, limiting their application.

Since microwires only record activity through the exposed electrode tip, increasing the number of electrodes to enhance recording sites results in larger electrode sizes and more significant tissue damage. Microelectrode arrays are composed of ordered or disordered integrations of multiple microelectrodes, and the diffusion layer between each electrode does not overlap. The current intensity and detection sensitivity can be improved. Thomas *et al.*[22] reported the first microelectrode array in 1972, which could record LFP signals but could not obtain the electronic signal of a single neuron. With changes in the electrode structure and development of technology, the APs of cells can be recorded, and the recording time can be extended. Meanwhile, nanomaterials have been applied to measure the signals of individual cells/neurons. Kawano and co-workers[23] presented a three-dimensional nano-scale electrode tip of a microelectrode array with a high aspect ratio.

2.2 Glass microcapillary

A glass microcapillary consists of a glass shell, metal lead, and a tip made of a special material (usually platinum, silver, stainless steel, or tungsten) filled with an electrolyte solution. The capillary glass tube is generally heated and stretched to produce a tapered tip as fine as a few microns in size. It is then filled with a conductive solution that allows good electrical conductivity between the tissue being recorded and the acquisition device. When the tip touches the surface of the neuron, its firing activity can be recorded. Glass microcapillaries are simple to prepare and their tip size is easy to control. These have been widely used in neuroelectrophysiological experiments, such as membrane clamping, but their physical and electrical properties are poorly reproducible and unsuitable for long-term use.

2.3 Silicon-based microelectrodes

The development of microelectromechanical systems and microfabrication technologies has facilitated the development of silicon-based microelectrodes.[27] The integration of electrodes can improve signal reliability, while the miniaturisation and homogenisation of electrode size helps overcome the limitations of microwire electrodes. In addition, the production of rigid materials on the wafer scale reduces electrode buckling. Michigan and Utah silicon-based microelectrodes are the two most commonly used types.

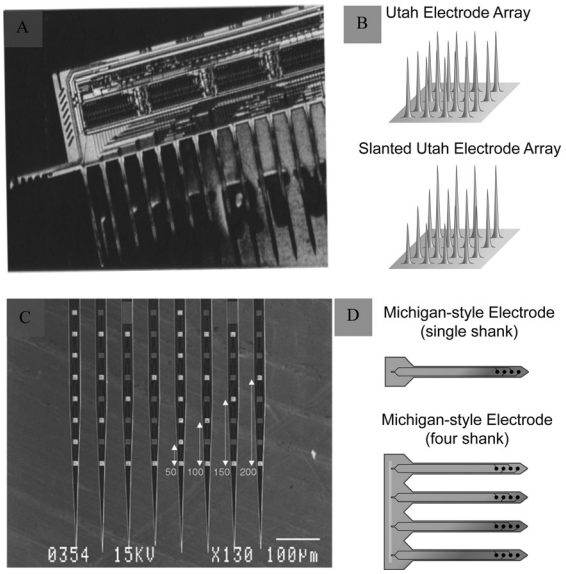

Fig. 4 Michigan and Utah electrodes and their schematics. (A) Michigan electrode. Reproduced with permission from ref. 31. (B) Schematic representations of an Utah electrode (adapted from ref. 26). (C) Utah electrode. Reproduced with permission from ref. 32. (D) Schematic representations of a Michigan electrode (adapted from ref. 26).

Michigan microelectrodes were first reported by Wise *et al.*[15] in 1970 at the University of Michigan. They were designed using an in-plane scheme, in which the microelectrode recording sites, pads, and leads were located within a single face of the microelectrode rod printed on a silicon substrate (Fig. 4A and B). The exposed microelectrode recording sites are generally squares with side lengths of several tens of micrometres. There are multiple acquisition sites distributed on a silicon microelectrode, which are generally used for recording spikes or LFP signals in an animal's skull. Based on this, the electrodes have undergone a series of improvements and processing and can be fabricated into three-dimensional neural microelectrodes, which can achieve up to 1024 channels of simultaneous recording.[28]

Another Utah silicon-based microelectrode, developed by Normann, is structurally different from the Michigan microelectrode. It uses an out-of-plane design in which the recording site is a raised needle-like tip, usually consisting of 25–100 small probes, each about 80 μm long and 1500 μm in diameter (Fig. 4C and D). Utah microelectrodes are widely used to record neurons in the animal brain. It is the only electrode that has been implanted into the human brain. It was applied in clinic and provided a significant advancement in neurotechnology to enhance autonomy for individuals suffering from paralysis.[29,30]

Although microelectromechanical system technology has greatly enhanced the performance of silicon-based microelectrodes, the large mismatch between the ultrahigh mechanical modulus of silicon-based semiconductors and that of the soft

tissue limits the performance of the electrodes. The Young's modulus of brain tissue is between 10^3 and 10^4, whereas silicon-based electrodes have a Young's modulus ranging from 10^{11} to 10^{12}. The bending stiffness of brain tissue is between 10^{-14} and 10^{-12}, in contrast to silicon-based electrodes, which range from 10^{-4} to 10^{-6}.

2.4 Polymer electrodes

The mismatch between the mechanical properties of electrodes made on rigid substrates, which are stiffer than biological tissues (*e.g.*, silicon), can trigger an inflammatory response involving glial cells and the diffusion of cytokines during chronic recording of the brain, leading to the formation of a glial scar around the electrode.[33] The inflammatory response acts as an insulator at the border, leading to electrode failure. To avoid this mechanical mismatch, polymer electrodes with low Young's moduli and good biocompatibility can be used.

Polyacetylene, polyparaphenylene, polyaniline,[34] polypyrrole,[35] and polythiophene[36] are five commonly used conductive polymers, SU-8[37] is also a type of polymer (Fig. 5A). These polymer materials exhibit good mechanical properties. As active or composite materials, they can be used as promising components of electrodes. The conductor part of the polymer electrode is made of one or more thin metal layers (200–300 nm thick), located between the polymer substrate and the encapsulation layer, thereby forming a ''sandwich'' structure that exposes the area of the site in contact with the brain tissue and the area connected to the lead through laser opening or ion reaction. In addition, as an organic conductor, the conductive polymer poly(3,4-ethylenedioxythiophene):poly(styrene sulfonate) (Fig. 5B) has high conductivity, stability, and transparency, and is also widely used in the preparation of electrodes. Conductive polymers exhibit high conductivity, high specific surface area, and good environmental stability. Moreover, the characteristics of a conductive polymer vary significantly with the doping material, and the electrical characteristics can be adjusted from that of an insulator to that of a conductor. Owing to their organic molecular structures, polymers can easily combine with active molecules in human bodily fluids and exhibit excellent biocompatibility (Fig. 5C).

However, the impedance and electrochemical stability of conductive polymer coatings are important factors that limit their service life. As the implantation time increases, the dopant migration from the conductive polymer coating degrades the electrochemical performance of the electrodes. In addition, owing to the poor long-term stability of conductive polymers, their electrical activity decreases linearly over time in non-corrosive environments.[38]

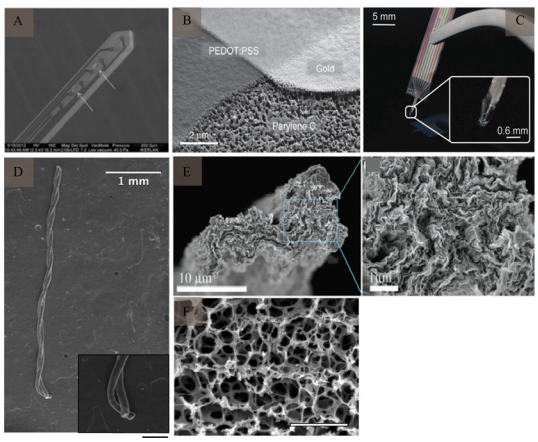

Fig. 5 Polymer electrodes and CNTf microelectrode. (A) Flexible SU-8-based electrode. Reproduced with permission from ref. 53. (B) SEM image of PEDOT:PSS electrode patterning. Reproduced with permission from ref. 54. (C) Flexible parylene sheath neural probe. Reproduced with permission from ref. 55. (D) SEM image of two-channel CNTf microelectrodes; inset shows CNTfs only at the electrode tip (scale bar: 200 μm). Reproduced with permission from ref. 42. (E) SEM images of graphene microfibers; enlarged SEM image shows aligned characteristic features of graphene microfibers. Reproduced with permission from ref. 56. (F) SEM image of the porous surface of the graphene material (scale bar: 2 μm). Reproduced with permission from ref. 57. CNTf, carbon nanotube fibre; CNT, carbon nanotube; SEM, scanning electron microscopy; PEDOT, poly(3,4-ethylenedioxythiophene); PSS, poly(styrene sulfonate).

2.5 Carbon-based nerve electrodes

The good electrochemical stability, capacitive mechanism,[39] as well as, chemical inertness and biocompatibility of carbon materials[40] make them ideal neural materials. In addition, their small size can significantly reduce immune reactions between the electrodes and tissues.

Carbon-based nerve (CNT) fibres (Fig. 5D) have received considerable attention for use at neural interfaces, because of their good biocompatibility and excellent mechanical, electrical, and chemical properties.[41,42] Meanwhile, they possess high specific surface area (700–1000 $m^2\ g^{-1}$),[43] ultra-high mechanical strength (individual carbon tubes have an elastic modulus of about 1 TPa).[44] Compared to conventional metal microwire electrodes, CNT fibres exhibit less tissue immunoreactivity. Fewer astrocytes and microglia were found around CNT electrodes, as compared to those around platinum–iridium alloys, indicating a smaller immune response in the tissues. CNTs have also been widely used as coatings for nerve electrodes, to enhance their conductivity and specific surface area. Despite these advantages, the potential cytotoxicity of CNTs needs to be further investigated,[45] especially in the field of human healthcare. Nanomaterials' ability to penetrate the blood–brain barrier can lead to irreversible neuronal damage.

Similar to CNT, graphene (Fig. 5E and F) has been extensively studied because of its excellent mechanical properties (elastic modulus $\approx$ 1 TPa),[46] electrical properties (electrical conductivity = 1 S m^{-1}), thermal conductivity (3000 W m^{-1} K^{-1}),[47] and good chemical stability and biocompatibility. Graphene has a higher specific surface area than CNT,[43,48] indicating that it exhibits lower cytotoxicity at high concentrations.[49] Kim *et al.*[50] discussed the production of graphene through a revised version of the Hummers' method and its use in detecting dopamine through electrochemical means. Additionally, graphene oxide and reduced graphene oxide have been recognized as promising for inhibiting microbial infections.[51] Another study[52] highlighted that collagen and graphene-based composites act as a flexible neurotrophic

platform, achieving a balance between biocompatibility and physiologically relevant conductivity, while also offering strong mechanical properties. Additionally, the low double-layer capacitance of single-layered graphene can result in thermal noise and a low SNR in neural recordings.

2.6 Flexible electrodes

In addition to the inflammatory response caused by the mismatch of the Young's modulus, rigid electrodes can also cause mechanical damage and displacement, which cannot adapt to the growth of brain tissue during long-term implantation and limit its functional expansion. Therefore, there is a need to develop flexible electrodes to overcome these limitations. Tang *et al.*[58] divided flexible electrodes into flexible, stretchable, and low-modulus electrodes. Among them, the use of ultraflexible[59] (Fig. 6A), mesh-like[60] (Fig. 6B), and fiber-like[61] (Fig. 6C) electrodes can better fit the characteristics of the brain tissue to achieve a better match, reduce the immune response, and enhance their stability to record the APs of single cells for a long time. In addition, because of the dynamic developmental process of brain tissue, especially volume changes, flexible electrodes with extensibility can adapt to changes in the brain tissue, which is mainly achieved by stretchable structures and materials[60,62] (Fig. 6D and E), such as hydrogel. Natural biomaterials have an elastic modulus similar to that of the brain tissue and are mostly porous in structure, thus making them ideal materials for the preparation of flexible electrodes. A research[63] reported the results of a neural interface using hydrogel as an ionic conductor and elastomers as dielectrics

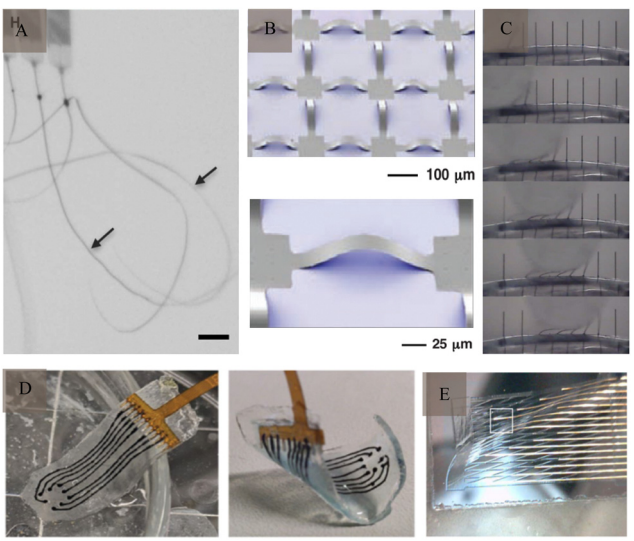

Fig. 6 Flexible electrodes. (A) Ultraflexible nanoelectronic probes, arrows indicate the probes (scale bar: 100 μm). Reproduced with permission from ref. 59. (B) Stretchable silicon membrane integrated on elastomeric substrates and enlarged image. Reproduced with permission from ref. 60. (C) Silicone-embedded carbon fibres in bend test. Reproduced with permission from ref. 61. (D) Viscoelastic array made of hydrogel (scale bar: 3 μm). Reproduced with permission from ref. 71. (E) A mesh electrode after being released from its silicon wafer. Reproduced with permission from ref. 62.

demonstrating that it induced a much smaller glial response and damage to cerebral blood vessels compared to metal electrodes. In addition to flexible electrodes, such as polymer- and carbon-based electrodes, nanomaterials represented by nanocellulose offer many advantages such as abundant sources, high mechanical strength, high polymerisation, high crystallinity, and good biocompatibility. Gao *et al.*[64] presented self-assembled arrays of electrode nanofilms had the capability to establish close and interconnected connections with neural tissue, facilitating consistent recording of neuronal activity. Seo *et al.*[65] reported on a high-density, flexible neuroelectronic array, with its signal recording accuracy verified through rat experiments.

However, its application also faces many challenges. The primary challenges with flexible electrodes for chronic recording include their low bending stiffness and insertion difficulties. To address these issues, adjustments to the electrode's surface coating were made to alter its stiffness. This modification aimed to buffer electrode-tissue interactions by increasing surface roughness, enhancing mechanical flexibility, and improving information transmission accuracy. A research[24] demonstrated the use of ultrasoft microelectrodes, inserted and removed with a polyethylene glycol (PEG) adhesive-coated stainless steel shuttle. Lo *et al.*[66] reported that an ultrafast degrading tyrosine-derived polycarbonate coating could provide sufficient stiffness for electrode insertion. Kil and colleagues[67] developed dextran as a coating material to improve the mechanical strength of flexible electrodes. Agorelius *et al.*[68] presented an implantable array of extremely thin electrodes, encapsulated in a firm yet soluble gelatin-based material, maintaining structure upon insertion. Sharafkhani *et al.*[69] devised a method for creating a neural microprobe with binary stiffness compliance, assessing its equivalent elastic moduli, critical buckling force, and brain tissue strain due to micromotions. Another research[70] evaluated the use of a thin extracellular matrix protein layer as a biodegradable coating to temporarily reinforce delicate or highly flexible thin-film neural implants for brain placement. Following the implantation process, they softened and provided interfaces that could adapt dynamically.

2.7 Optical probes and injectable optoelectronics

In addition to traditional electroneural recordings, probes have also been designed ecogniise genetic tools for optical neuromodulation.[72] With the advent of optogenetics, it has become possible to excite or inhibit geneticalecognizableble cell types by expressing light-sensitive proteins (Fig. 7A). Optogenetic experiments typically require the implantation of multifunctional devices for light stimulation, delivery of viral vectors and drugs[73] (Fig. 7B), and simultaneous recording of electrophysiological signals from specific cells within the nervous system.

Here is a list of highly cited literature on materials, technologies, biocompatibility and surface modifications related to neural implantable microelectrodes since 2010 (Table 1).

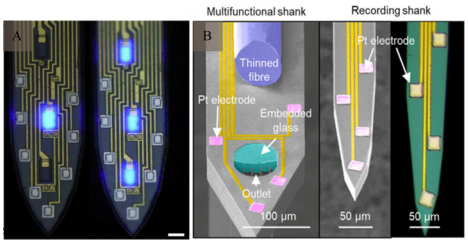

Fig. 7 Optical probes and injectable optoelectronics. (A) High-magnification images of the illuminated micro light-emitting diodes (scale bar: 15 μm). Reproduced with permission from ref. 74. (B) A multifunctional, implantable optoelectronic device. Reproduced with permission from ref. 75.

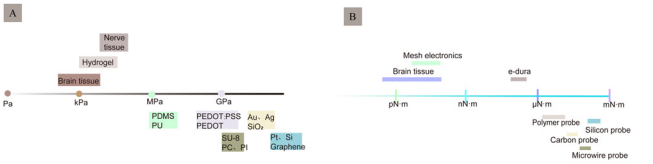

Fig. 8 Young's modulus and stiffness of different materials. (A) Young's modulus of different materials. (B) Stiffness of different materials. PC: parylene-C; PI: polyimide; PDMS: polydimethylsiloxane.

3. Current challenges in biocompatibility and electrochemical properties in electrodes

Despite advancements in signal resolution, signal density, and biocompatibility, the development of implantable neurological recording electrodes, especially rigid electrodes, encounters numerous challenges. Notably, the discrepancy in the modulus of elasticity between rigid metals (GPa) and soft brain tissue (kPa) and the variability in electrode rigidity present significant issues (Fig. 8). This mechanical mismatch between electrodes and brain tissue can cause electrode rejection and displacement, negatively impacting biocompatibility and the stability of long-term neural recordings.[82,83] Moreover, the electrochemical properties of electrodes influence signal quality, with traditional metallic materials compromising signal integrity due to high impedance, low charge injection capacity, and limited surface area. This section outlines the current challenges regarding electrodes' biocompatibility and electrochemical attributes.

3.1 Biocompatibility

As a foreign body implanted in the brain tissue, electrodes are in direct contact with the nervous system. Traditional electrodes are mostly rigid electrodes made of metal materials whose elastic modulus differs greatly from that of the brain tissue; owing to which they cannot achieve better mechanical and geometric adaptation with the brain tissue. There are risks of infection and rejection as well involved with these, which easily causes instability and displacement of the electrode, thus making it difficult to achieve a safe and reliable connection with the tissue. The biggest challenge faced by the nerve-electrode interface is the biocompatibility of electrodes.[84,85]

Table 1 Highly cited literature related to neural implantable microelectrodes

Review	Year	Summary	Citations
Hydrogel bioelectronics[76]	2019	This review examines the fundamental mechanisms of interactions between tissue and electrodes, the distinct advantages of hydrogels in interfacing with the human body, recent advancements in hydrogel development for bioelectronics, and provides rational guidelines for the design of future hydrogel bioelectronics.	647
Materials and technologies for soft implantable neuroprostheses[77]	2016	The review underscore the significance of reducing the disparity in physical and mechanical properties between neural tissues and implantable interfaces, the potential material-based approaches for the development and production of neurointegrated prostheses, and delineate their therapeutic promise.	411
A review of organic and inorganic biomaterials for neural interfaces[78]	2014	This paper provides a review of cutting-edge microelectrode technologies. It examines the progress made in electroactive nanomaterials and addresses the technical and scientific obstacles related to biocompatibility, mechanical incongruity, and electrical properties that these nanomaterials encounter in the pursuit of creating durable and effective neural interfaces.	407
Neural recording and modulation technologies[27]	2017	This review examines the design principles derived from the field of neural engineering, which has been established. Furthermore, it emphasizes recent advancements in neural probes driven by materials innovation and explores emerging directions influenced by the principles of neural transduction.	344
Polymers for neural implants[79]	2011	This study centers on the neuro-technical interface and provides an initial overview of its essential characteristics. It offers a description of the prevalent polymer materials and their properties. It concludes by outlining various applications and their distinct designs, along with the associated manufacturing techniques.	336
Glial responses to implanted electrodes in the brain[80]	2017	The work proposes a shift in the conventional perception of glia as a static obstacle, and examines their function as an influential factor in the results of device implantation. Furthermore, it explores the potential implications of this perspective on the advancement of bioelectronic medical devices.	305
Next-generation probes, particles, and proteins for neural interfacing[81]	2017	The review delineates the impact of advancements in the comprehension of neural signaling and material-tissue interactions on the diversification of available tools. Novel probe designs and materials are extending the boundaries of recording and stimulation capabilities in terms of longevity, localization, and specificity, thereby challenging the distinction between living tissue and engineered instruments	301

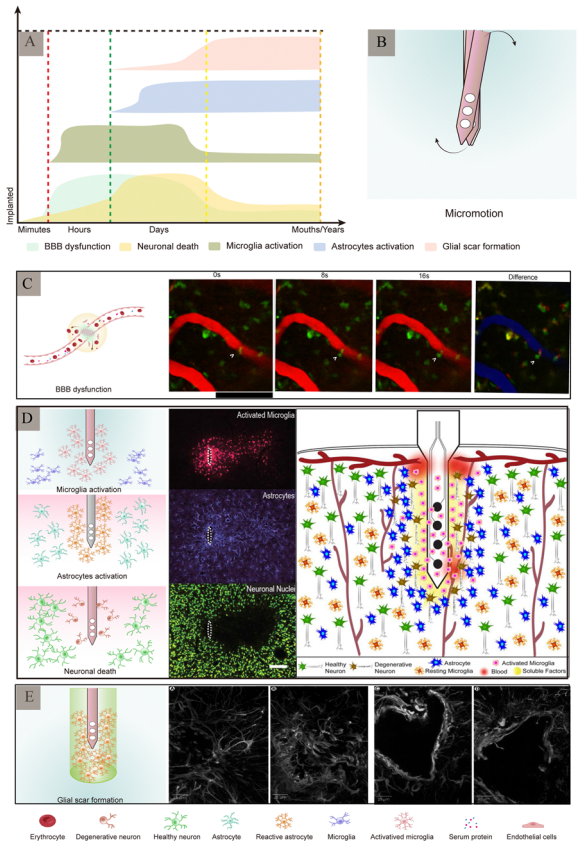

Fig. 9 Major pathological changes in the brain after electrode implantation. (A) Different stages of inflammatory response and main pathological changes after electrode implantation (adapted from ref. 90). (B) Micromotion of the electrodes in the brain tissue after implantation. (C) Leakage of the blood–brain barrier. Arrow indicates cell in the blood–brain barrier squeezing through the endothelium into the central nervous system. Reproduced with permission from ref. 91. (D) Schematic diagram of the major rejection reactions after electrode implantation and immunofluorescence staining of the related cells. Reproduced with permission from ref. 26. (E) Glial scars formed by astrocytes at different time-periods after electrode implantation. Reproduced with permission from ref. 89.

A series of rejection reactions, including acute and long-term reactions, occur in the tissue after electrode implantation (Fig. 9A). In addition, brain tissue damage can also occur due to displacement of the electrodes in the brain tissue after implantation (Fig. 9B). Acute reactions are mainly due to mechanical damage caused by electrode implantation into the cortex and the subsequent inflammatory reaction.[86] Astrocytes and microglia are the primary cells that elicit injury responses in the brain. Early on, there is an increase in the number of astrocytes and microglia around the electrode, and the inflammatory molecules produced by the microglia cause neuronal cell death and activate astrocytes,[87,88] which change shape and engulf the electrode. In contrast, on the other hand, blood-derived macrophages disrupt the BBB and enter the damaged vessels[84] (Fig. 9C). When the electrode is implanted for a few weeks, the acute foreign body reaction disappears, followed by a chronic foreign body reaction mainly manifested by the appearance of reactive astrocytes,[83] microglial activation (Fig. 9D), and glial scar formation[89] (Fig. 9E). During this time, astrocytes surround the electrode around the tissue and grow on its surface to form a tight protective sheath or fibrous encapsulation that isolates the electrode from the tissue such that the two cannot effectively contact each other. The glial scar, which insulates the electrode from nearby neurons, while separating the damaged tissue from the healthy tissue, to maintain the BBB, prevent lymphocyte infiltration of the barrier, prevent signal expansion, and increase impedance.

Electrode shape, size, and material all have an impact on biocompatibility. The shape of the electrode tip may not only affect the surrounding cellular response, but also affect its stability after implantation. The specific shape design[92] can reduce the displacement between the probe and brain, reduce the inflammatory response, and enhance the stability of signal recording (Fig. 10A). Innovative shapes like flexible filamentary probes,[93] sheet-like architectures[94,95] and mesh-like geometries[96] have been developed to improve biocompatibility. In addition, 3D structures are being employed for electrodes.[97,98] On the other hand, when a foreign body is implanted in the brain tissue, the electrode causes mechanical damage to the brain tissue; the larger the electrode size, the more damaging it will be. It also causes glial cell proliferation, which in turns affects the quality of signal recording and duration of signal acquisition. Implanting electrodes with smaller cross-sectional areas can reduce tissue damage,

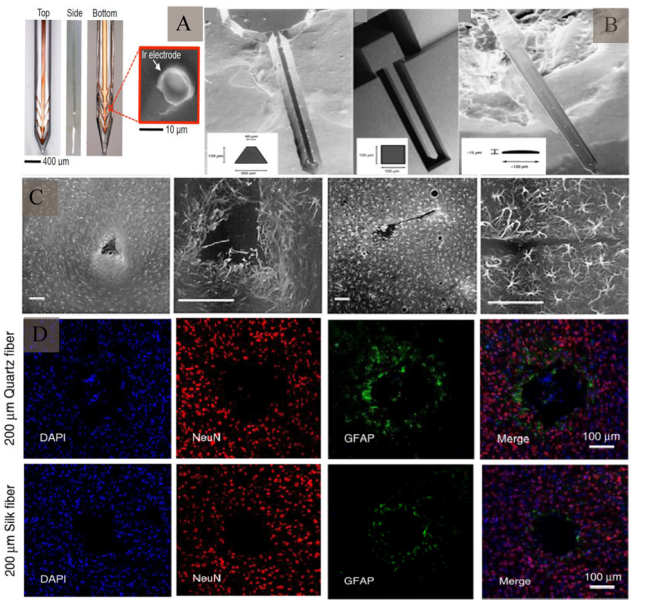

Fig. 10 Intracerebral tissue changes induced by electrode structures of different shapes and sizes. (A) Electrodes with anchor protrusions designed to reduce displacement after insertion into the tissue. Reproduced with permission from ref. 92. (B) Scanning electron microscopy images of electrodes with different shapes and sizes, formed using different preparation methods. Reproduced with permission from ref. 86. (C) Effect of electrodes with different cross-sectional areas on astrocytes, at 1 week after implantation. Reproduced with permission from ref. 86. (D) The effect of electrodes made of different materials on neurons and astrocytes, after implantation. Reproduced with permission from ref. 101.

including harm to vascular and local neuronal environments due to device insertion, and improve mechanical compliance with brain tissue as well as the spatial resolution of the electrode. Immunofluorescence staining of silicon probes of different shapes one week after implantation into brain tissue showed that 1 week after implantation, silicon probes with larger cross-sectional areas displayed higher positive cell density and hypertrophy of astrocytes than smaller electrodes[86] (Fig. 10B and C).

In addition, the difference in stiffness between the brain tissue and the implanted neural probes is a likely source of tissue damage. The probes made of soft materials can mitigate adverse damage and immune responses (Fig. 10D). In one study, implantation of a flexible poly(polyparylene) probe within 75 μm resulted in 12–17% neuronal loss around the implantation site, whereas implantation of a rigid silicon probe within 100 μm resulted in 40% neuronal loss after implantation.[99] Moreover, electrode arrangement spacing[100] also affects glial cell proliferation.

3.2 Electrochemical performance

Electrochemical reactions and double-layer charging make up the electrode/electrolyte border for electrophysiological recording.[102,103] In terms of electrochemical performance, conventional electrodes based on metal materials affect the quality of their signals due to their high impedance, low charge injection capability and low surface area.

The quality of the SNR is the main factor affecting signal recording; the lower the SNR, the lower is the information on the effective neurons of the signal. To increase the SNR, it is necessary to reduce the noise amplitude while increasing the signal strength.[104] The noise sources in neural signal recording include three main aspects: the noise of the electrode itself, background noise of the neuron, and noise in and around the recording system, especially the 50/60 Hz power-line frequency interference. The noise introduced by the electrode itself is primarily thermal noise, which is the electronic noise generated upon thermal perturbation.[105] The magnitude of the thermal noise is unrelated to the applied voltage, but is related to the impedance. The thermal noise is directly related to the square root of the resistance of the electrical double-layer formed at the electrode/electrolyte interface. Biological background noise is the main source of noise in cortical recordings and is the sum of APs outside other nerve cells in proximity. The electrode impedance, density of surrounding neurons, and frequency of neuronal discharges have a significant effect on biological background noise. With respect to external noise, 50/60 Hz power-line frequency interference is one of the most serious disruptive factors in recording electrical signals. There is also equipment noise, such as that from amplifiers. The higher the power consumption and larger the area of the amplifier, the higher the noise. The electromyogram signal also affects extracellular APs, and the filter band needs to be reasonably adjusted in this scenario. Moreover, the photoelectric effect during light stimulation,[106] motion-induced signal artefacts, and immune response-induced electrode insulation[107] influence electrical signals.

A fundamental requirement for an ideal implant is to acquire as many neurodynamic signals as possible from the target neuron, in the absence of background noise. In addition to decreasing disturbances to the environment and equipment by shortening the length of the recording electrode connection, reducing the system size, shielding the circuit as much as possible, and improving the performance of the electrodes can serve as effective methods.

In terms of improving the stability of the electrode, achieving long-term stability of the signal requires not only needs the stability of the electrode itself, but also that of its tissue-level mechanical properties, which can resist long-term corrosion of the physiological environment in the brain, in addition to offering good electronic properties such as high conductivity, resistance to the penetration of ions and water, overcoming the influence of the internal environment, and maintaining stability in the extracellular fluid environment. In addition, the recording electrodes used for implantation rely on limited equipment to achieve signal extraction and analysis, and overcoming the wire connection in the collection and recording of neural signals can greatly improve the ease and comfort of operation.[108]

4. Progress and outlook

Although the performance of electrodes is constantly improving, there are still some obstacles and challenges in achieving high-throughput, multi-mode, and multi-region recordings of neurons while simultaneously minimising brain tissue damage. The electrode should maintain good electrical, chemical, and mechanical properties under the premise of high biocompatibility, to achieve accurate and stable signal recording. The performance of an electrode is affected by various factors upon implantation into the neural tissue. It is subject to the *in vivo* interaction of the above factors, thus resulting in a complex relationship network. This increases the challenge in improving the performance of neural electrodes. Improving the overall electrode performance without affecting other factors is an urgent issue that must be addressed, related studies have made progress in this regard.

Traditional implantable probes encounter challenges due to their stiffness not aligning with biological tissues and the difficult balance between transparency and electron conductivity. Liang *et al.*[109] reported conductive and transparent hydrogels using polypyrrole-decorated microgels as crosslinkers. In harmonising the biocompatibility and conductivity of electrodes, Kim and co-workers[110] introduced a neural interface composed of a supramolecular β-peptide-based hydrogel, which is biocompatible, conductive, and biostable. This hydrogel facilitates signal amplification through close neural/hydrogel contact without inducing neuroinflammation. Zhang *et al.*[111] developed a reliable method for integrating traditional electrodes with conducting hydrogel coatings, mirroring tissue

properties, including favorable electrochemical performance. Regarding the functional integration of electrodes, a versatile multi-shank MEMS neural probe was developed, integrating an optical waveguide for optical stimulation, microfluidic channels for drug delivery, and microelectrode arrays for recording neural signals from various cellular regions.[112] Lanzio *et al.*[113] demonstrated the production of a multifunctional neural probe with compact shank dimensions, high sensor density, and the ability to focus light within deep brain tissue, Chen and co-workers[114] engineered electrode materials by incorporating polypyrrole nanowires onto highly conductive polypyrrole electrode arrays. This innovation allows for the creation of stretchable polymeric microelectrode arrays (MEAs) featuring high stretchability, robust electrode-substrate adhesion, low Young's modulus, and high conductivity. In addition, Neurotassel[115] and Neural Matrix[116] have provided support for achieving flexibility, high resolution, and stability in electrode recording. Based on a combination of electrode performance and brain tissue environment, achieving the optimisation of the recording signals, improvement of biocompatibility, accuracy of cell-specific recording, functionalisation of electrode performance are future directions for electrode modification (Fig. 11).

4.1 Optimisation of the recording signals – high quality, high resolution, low noise, and long time range

Reducing the electrode size to the greatest possible extent is important for reducing the rejection reaction and improving the efficiency/stability of signal recording. However, with the continuous updating of recording electrodes, more stringent requirements have been proposed for high-throughput electrode recording signals.

It has been reported that a neural interface of 3075 channels composed of 192 fibres can achieve high density information collection.[117] The problem of increasing electrode size must be overcome by increasing the electrode flux. The size of the electrode can be controlled within a certain range using a microelectromechanical system and complementary metal oxide semiconductor. Further developments in miniaturised integrated electrodes are now available, for example, the silicon probes-neuropixels.[118] Each probe features 384 recording channels that can target 960 low-impedance TiN6 sites, compatible with complementary metal–oxide–semiconductor processing. Its compact size and integrated functionality allow for the recording of vast neuron populations. Vomero *et al.*[119] prepared polyimide-based flexible intracortical devices capable of being manufactured at dimensions smaller than a human hair. Melosh and co-workers[120] developed an electrode connector using a highly flexible thin-film electrode array, Flex2Chip, which autonomously aligns with silicon microelectrode arrays, enabling the integration of thousands of channels within a millimeter-scale framework. It has been shown that 65536 channels can be integrated into a single microwire electrode.[121] However, when the size of the electrode increases to a certain extent, the signal amplitude received by the electrode tends to average; therefore, it can only reflect the LFP activity of the neural population.[122] To achieve high-flux and -density recording of the electrode, it is necessary to record a large number of neurons and understand the interaction of neurons simultaneously to improve the resolution of individual neuron recognition and detection.

To improve the SNR, it is necessary to adjust the interface impedance so that the electrode can obtain a larger exposed surface area within a limited size range. The application of metal, metal nitride, and carbon composite materials[123–125] can increase the electrode surface area, improve electrode conductivity, stability, and other electrochemical properties. The conductive nanomaterials can improve the SNR by providing more efficient surface area;[126] the ultrathin flexible electrodes made of polyimide electrodes (75 μm) maintain a high SNR, with great conformal contact of nearly all channels.[75] Kim *et al.*[127] showed that 2.5 μm mesh electrodes exhibit an SNR that is 5.7-fold that of polyimide electrodes. The use of electrodes made with CNT[128] composite coatings and graphene electrode after steam plasma processing[129] could improve the SNR; in other words, an improvement in the material can improve the SNR. On the other hand, the micromotion of the electrode influences the SNR, Kipke *et al.*[130] reported that silicon-substrate microelectrodes with a printed circuit board on flexible polyimide ribbon cables could provide high-quality neural signals with a high SNR. In addition, surface modification of electrodes is an important means of improving the electrochemical properties of electrodes.

Electrochemical modification of electrodes mainly consists of two types: one involves increasing the bilayer capacitance of electrodes by roughening the electrode surface or using materials with larger specific surface areas to increase the electrochemical surface area of electrodes, such as porous treatment of electrodes or using materials such as CNTs/graphene.[131] In this way, no electrochemical reaction occurs during charge transfer, and the stability of the electrode in use can be improved. However, this method has the disadvantage of a small charge capacity. Another method involves modifying the electrode by using materials with Faraday pseudocapacitance properties such as iridium oxide[132,133] conducting polymers. However, the different methods for preparing iridium oxide have different limitations, such as high cost and electrode shape requirements. In addition, conductive polymers are more commonly used for the modification of nerve electrodes. Pyrrole and thiophene are commonly used conductive polymer

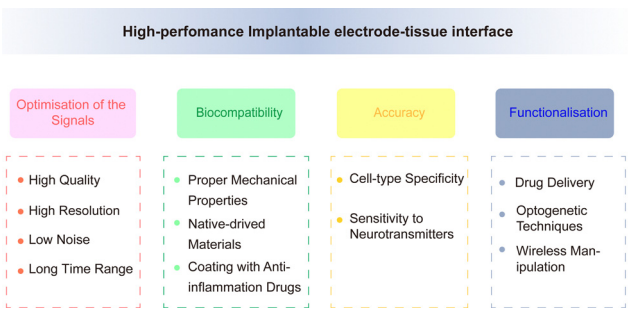

Fig. 11 Properties of an ideal implantable electrode-tissue Interface.

materials for the modification of electrodes.[134] Conductive polymers can be realised by doping different ions into the body to improve the electrode performance; doping polyphenylene sulfonic acid sodium and tetraethylammonium perchlorate as counter ions into the conductive polymer can reduce the impedance of the electrode,[135,136] while doping bioactive molecules such as heparin, nerve growth factor, and hyaluronic acid into the conductive polymer can alleviate the inflammatory reaction caused by electrode implantation and promote the adhesion and differentiation of neurons on the electrode surface.[137,138] PEDOT:PSS and iridium oxide coatings can lower the interfacial impedances of gold electrodes for electrophysiology across various sites.[117]

Nanomaterial modifications play a crucial role in enhancing the electrochemical properties of implantable electrodes. Nanoparticle deposition on electrodes can enhance the surface-area-to-volume ratio, reducing impedance and minimizing noise interference.[139] Shi *et al.*[140] presented composite films made of uniform single-walled carbon nanotube/PEDOT with nanoscale pores and microscale grooves, significantly increasing the interface between the electrode and electrolyte. The microelectrode modified with Au hierarchical nanostructure demonstrated a significant enhancement of approximately 9.79 dB in SNR compared to the bare electrode.[141] A research[142] introduced a neural probe design focusing on a polymer nanocomposite that mechanically softens and is inspired by biology, exhibiting stable electrochemical impedance spectra. Liu *et al.*[143] reported that nanozyme-based neural electrodes can perform multiscale and ultrasensitive neural recording, with low resistance (26 times lower than conventional metals), high sensitivity (10 times higher than PtIr electrodes for field potential recording), and high SNR (14.7 dB for single-neuron recordings in rats). Wang and colleagues[144] introduced a dual-layer platinum black-PEDOT/PSS coating that enhances recording stability and SNR, with particular effectiveness in reducing photoelectric artifacts.

4.2 Improvement of biocompatibility

Currently, research on electrode development is focussed on gradually achieving higher similarity with the nerve tissue, in terms of mechanical properties, shape, and other aspects.

To improve biocompatibility, researchers are focusing on optimising electrode materials, shapes, and surface modification materials. With respect to materials, the electrode performance is constantly optimised to better fit the biological state of the brain tissue, reduce the immune response, and improve the traditional rigid probe. On the one hand, materials with a low Young's modulus, as that of the electrode base, such as polyaniline, polyimide,[145,146] parylene[94] and other flexible and conductive polymers, graphene[147] and other two-dimensional carbon nanomaterials (with high electrical conductivity, mechanical flexibility, and good biocompatibility in a single atomic layer thickness), and SU-8, *etc.*[148,149] can be used. The Neuralink array[117] has 3072 sensing sites that are spread across 96 distinct soft filaments. These filaments can move with brain tissues during breathing and pulsatile blood flow, and reduce neural damage and glial scar formation. A study[150] presented flexible microelectrode arrays characterized by enlarged surface areas, a high density of electrodes, and distinctive self-unfolding capabilities, which have been documented to facilitate minimally invasive implantation of visual prostheses. Gao *et al.*[151] developed highly flexible and stretchable MEAs by utilizing free-standing carbon nanotube network embroidered graphene films as recording microelectrode. The use of flexible materials with an elastic modulus similar to that of the brain tissue improves the overall design of the electrode; examples of the same include micro-flexible electrodes, nerve tassel electrodes, and syringe electrodes, which can not only reduce the immune response during implantation but also change into a substance with a Young's modulus similar to that of the brain tissue upon insertion. Hydrogels have viscosity, elasticity, and other mechanical properties that are similar to those of the brain; these properties aid in reducing rejection. Studies have shown that human neural progenitor cells can be transformed into various specific cell types by implanting hydrogels into scaffolds, which can form a network of lattice-like structures and differentiate into various cell types with specific characteristics. Astrocytes and oligodendrocytes contribute to tissue repair and electrode function with the goal of realising long-term signal recording. Recent studies have reported[152] a way of fabricating electrodes in living tissues, which involves injecting a gel into the organism through a series of biological reactions, eventually forming a soft and conductive polymer gel that greatly reduces tissue rejection. Conductive materials can also be implanted into biological tissues. Thus, it is possible to create neural electrodes that can be accepted by the brain tissue and immune system.

Sheet and reticular structures have been developed to adapt to the shape of the brain tissue. For example, biomimetic design[153] can be used to manufacture flexible electrodes with a single-neuron structure and mechanical properties that can maintain flexibility while providing a grid-like environment closer to the survival of neurons. The electrical and mechanical properties of the electrodes are further enhanced by surface modification.

The substrate is the main cause of inflammatory reactions in electrodes; therefore, improving the biocompatibility of the substrate is the main method to reduce rejection reactions. These modifications are primarily performed *via* surface coating, doping, and layer-by-layer self-assembly techniques based on electrostatic attraction and covalent grafting. Bahareh *et al.*[154] improved the biocompatibility of MEAs by coating the electrodes' surfaces with biocompatible polymers such as PEG and parylene-C. Hydrogels are commonly utilized in tissue engineering and drug delivery due to their ability to be customized to mimic biological tissue in terms of water content and mechanical properties. Cullen *et al.*[155] developed "living electrodes" by encasing living cortical neurons within soft hydrogel cylinders to record and modulate brain activity. Electrode arrays based on carbon fibers with silk supports were shown to elicit reduced glial reactions.[156] Hydrogels eluted with neurotrophic factors are used as coating materials for electrodes, to increase the affinity between the neurons and electrodes.

Spencer *et al.*[157] presented PEG hydrogels with tunable thickness and elastic moduli applied to neural probes, effectively reducing strain caused by micromotion around the implants. A research showed[158] that encasing a silicon microelectrode array with a thick hydrogel coating effectively reduced the long-term foreign body response 16 weeks post-implantation. Additionally, surface/neuron interfaces can be modified to control neural cell type-specific responses.[159] A research[160] presented a self-dissolvable microelectrode array, underpinned by a biocompatible and soluble material known as PEG. Upon insertion, the PEG dissolves in biological fluid, allowing the electrodes to detach and move freely within neural tissue. Doping bioactive absorbent molecules with biomaterials can save time and solve the surface adhesion problem, while modification using the layer-by-layer method can reduce the impedance change[161] and improve the biocompatibility of nerve cells.[162] Grafting can significantly reduce the inflammatory responses after electrode implantation.[163]

Nanomaterials have been widely used to mitigate adverse biological reaction. Boehle *et al.*[164] introduced a flexible approach to fabricate nanostructured platinum coatings with a large electrochemically active surface area, exhibiting favorable biocompatibility, low impedance, high charge injection capacity, and excellent long-term stability. Seker and coworkers[165] demonstrated that nano-porous gold surface coatings significantly reduce astrocyte coverage while maintaining normal neuron coverage. A research[33] indicated that implanted microelectrodes coated with Si nanopillars enhanced neuron survival compared to those with a microstructured surface.

4.3 Accuracy of cell-specific recording

Achieving specificity in electrode recordings, especially in terms of recognition of cell types, is also an important aspect of improving electrode performance. Photogenetic technology can achieve cell-specific regulation with millisecond accuracy. Simultaneously, the release of neurotransmitters can be controlled through the activation/inhibition of specific types of neurons (such as dopaminergic neurons) through photogenetic stimulation,[152] while sensitivity to the detection of neurotransmitter changes can be improved through the modification of metal nanoparticles, enzymes, and carbon-based materials. Lee *et al.*[166] introduced a hydrochromic sensor, suggesting its potential for visualizing implanted electrodes to monitor neurotransmitters or inflammatory responses. Currently, rigid electrodes are typically used to record neural activity in brain regions composed of thousands of neurons, whereas stretchable electrodes can record single cells for a long time, with millisecond resolution. Since they have cell type specificity, they can correlate the activity of specific neurons with related behaviours/feelings and further provide a basis for elucidating related neural coding mechanisms. Nevertheless, there is a need for further recognition of neuronal subunits for directional recording and modulation, through integration with multi-modal and multi-functional methods, integration of behaviourally defined cell types with molecularly defined cell types, and identification of biomarkers associated with neurological diseases.

4.4 Functionalisation of electrode performance

With progress in neuroscience research and emergence of new materials and technologies, electrodes are being developed for multiple functions, including simultaneously achieving drug delivery, electrophysiological stimulation, and recording, and can be combined with optogenetic manipulation[167] and other operations at the cellular level, to detect and intervene in nervous system activities, especially microfluidics technology.[168] Electrodes are now being developed for wireless manipulation, as adaptive probes to achieve long-term implantation, and for regulation of high spatial/temporal resolution of specific cells. Electrodes integrating flexible materials, optogenetic techniques, and drug delivery systems are already available.[169]

Implantable recording electrodes have a broad range of applications. Long-term stable connection and signal recording between the electrode and nervous system play an important role in neuroscience research and the diagnosis and treatment of neurological diseases, which can expand information sources, enrich treatment means, and improve treatment efficiency. The development of ion pumps and electrophoretic delivery devices has facilitated the development of electrodes for drug delivery, the capillary organic electronic ion pump (OEIP) facilitates the development of electrophoretic delivery devices with probe-shaped configurations, which are well-suited for transporting a range of ionic compounds.[170] Seitanidou *et al.*[171] reported the initial application of OEIP in mammalian cells or systems, illustrating the potential of this technology for enhancing the transportation and administration of various therapeutic agents at minimal concentrations.

In recent years, with the development of BCI, the technique has been used to treat seizures, reduce tremor in patients with Parkinson's disease, monitor the brain activity of patients with neurological diseases, restore the vision of the blind, and help patients with paralysis regain the feeling of limbs and even control things with their mind, using equipment, to achieve specific activities. With the development of computer performance, artificial intelligence, and the miniaturisation of implant devices, growing research on BCI has further improved its performance. In addition, many new technologies have been developed to achieve implant electrodes more safely and operably. In 2022, Doctor Magidi used Synchron's Strentrode™ to successfully perform a procedure to implant electrodes into blood vessels in the brain, to treat dyskinesia in patients with amyotrophic lateral sclerosis, with newer use of this technology significantly reducing tissue damage. With continuous improvement and optimisation of neural electrode performance, neural electrode implantation into the brain will enter the test stage of general application, and may even become a wearable neural technology for the diagnosis and treatment of human refractory diseases.

Author contributions

Kun Liu, Hao Zhang: conceptualization, writing – original draft. Minghui Hu, Zifa Li: writing – review & editing. Kaiyong Xu, Dan Chen, Wenqiang Cui, Cui L.: visualization. Sheng Wei,

Xiwen Geng, Ran Ding: conceptualization, funding acquisition, writing – review & editing.

Conflicts of interest

There are no conflicts to declare.

Acknowledgements

This work was supported by the National Natural Science Foundation of China (no. 81974553, 82004078, and 82274383), the Special Funding for the Taishan Scholars Project (no. tsqn202211137 and tsqn202211355), Natural Science Foundation of Shandong Province (no. ZR2020ZD17 and ZR2021LZY018), Natural Science Foundation of Tianjin City (no. 19JCQNJC11000), and Chinese Medicine and Brain Science Youth Scientific Research Innovation Team, Shandong University of Traditional Chinese Medicine (no. 22202101).

References

1 H. S. Mayberg, A. M. Lozano, V. Voon, H. E. McNeely, D. Seminowicz, C. Hamani, J. M. Schwalb and S. H. Kennedy, *Neuron*, 2005, **45**, 651–660.
2 R. Wennberg, M. Hodaie, J. O. Dostrovsky. and A. M. Lozano, *Epilepsia*, 2002, **43**, 603–608.
3 P. Krack, A. Batir, N. Van Blercom, S. Chabardes, V. Fraix, C. Ardouin, A. Koudsie, P. D. Limousin, A. Benazzouz, J. F. LeBas, A. L. Benabid and P. Pollak, *N. Engl. J. Med.*, 2003, **349**, 1925–1934.
4 A. A. Eshraghi, R. Nazarian, F. F. Telischi, S. M. Rajguru, E. Truy and C. Gupta, *Anat. Rec.*, 2012, **295**, 1967–1980.
5 J. R. Wolpaw, G. E. Loeb, B. Z. Allison, E. Donchin, O. F. do Nascimento, W. J. Heetderks, F. Nijboer, W. G. Shain and J. N. Turner, *IEEE Trans. Neural Syst. Rehabil. Eng.*, 2006, **14**, 138–141.
6 G. Buzsaki, C. A. Anastassiou and C. Koch, *Nat. Rev. Neurosci.*, 2012, **13**, 407–420.
7 J. Viventi, D. H. Kim, L. Vigeland, E. S. Frechette, J. A. Blanco, Y. S. Kim, A. E. Avrin, V. R. Tiruvadi, S. W. Hwang, A. C. Vanleer, D. F. Wulsin, K. Davis, C. E. Gelber, L. Palmer, J. Van der Spiegel, J. Wu, J. Xiao, Y. Huang, D. Contreras, J. A. Rogers and B. Litt, *Nat. Neurosci.*, 2011, **14**, 1599–1605.
8 K. Volkova, M. A. Lebedev, A. Kaplan and A. Ossadtchi, *Front. Neuroinform.*, 2019, **13**, 74.
9 A. Dubey and S. Ray, *J. Neurosci.*, 2019, **39**, 4299–4311.
10 B. Gunasekera, T. Saxena, R. Bellamkonda and L. Karumbaiah, *ACS Chem. Neurosci.*, 2015, **6**, 68–83.
11 Y. Jin, J. Chen, S. Zhang, W. Chen and X. Zheng, *Adv. Exp. Med. Biol.*, 2019, **1101**, 67–89.
12 H. L. Peng, J. Q. Liu, Y. Z. Dong, B. Yang, X. Chen and C. S. Yang, *Sens. Actuators, B*, 2016, **231**, 1–11.
13 M. V. Simon, M. R. Nuwer and A. Szelenyi, *Handb. Clin. Neurol.*, 2022, vol. 186, pp. 11–38.
14 Y. X. Kato, S. Furukawa, K. Samejima, N. Hironaka and M. Kashino, *Front. Neuroeng.*, 2012, **5**, 11.
15 K. D. Wise, J. B. Angell and A. Starr, *IEEE Trans. Biomed. Eng.*, 1970, **17**, 238.
16 F. Strumwasser, *Science*, 1958, **127**, 469–470.
17 J. D. Green, *Nature*, 1958, **182**, 962.
18 A. M. Dymond, L. E. Kaechele, J. M. Jurist and P. H. Crandall, *J. Neurosurg.*, 1970, **33**, 574.
19 C. M. Gray, P. E. Maldonado, M. Wilson and B. McNaughton, *J. Neurosci. Methods*, 1995, **63**, 43–54.
20 W. Pei, H. Zhao, S. Zhao, X. Fang, S. Chen, Q. Gui, R. Tang, Y. Chen, B. Hong, X. Gao and H. Chen, *J. Micromech. Microeng.*, 2014, **24**, 095015.
21 M. A. Nicolelis, D. Dimitrov, J. M. Carmena, R. Crist, G. Lehew, J. D. Kralik and S. P. Wise, *Proc. Natl. Acad. Sci. U. S. A.*, 2003, **100**, 11041–11046.
22 C. A. Thomas Jr, P. A. Springer, G. E. Loeb, Y. Berwald-Netter and L. M. Okun, *Exp. Cell Res.*, 1972, **74**, 61–66.
23 A. Goryu, R. Numano, A. Ikedo, M. Ishida and T. Kawano, *Nanotechnology*, 2012, **23**, 415301.
24 Z. J. Du, C. L. Kolarcik, T. D. Y. Kozai, S. D. Luebben, S. A. Sapp, X. S. Zheng, J. A. Nabity and X. T. Cui, *Acta Biomater.*, 2017, **53**, 46–58.
25 J. E. Ferguson, C. Boldt and A. D. Redish, *Sens. Actuators, A*, 2009, **156**, 388–393.
26 M. Jorfi, J. L. Skousen, C. Weder and J. R. Capadona, *J. Neural Eng.*, 2015, **12**, 011001.
27 R. Chen, A. Canales and P. Anikeeva, *Nat. Rev. Mater.*, 2017, **2**, 16093.
28 K. D. Wise, A. M. Sodagar, Y. Yao, M. N. Gulari, G. E. Perlin and K. Najafi, *Proc. IEEE*, 2008, **96**, 1184–1202.
29 J. L. Collinger, B. Wodlinger, J. E. Downey, W. Wang, E. C. Tyler-Kabara, D. J. Weber, A. J. C. McMorland, M. Velliste, M. L. Boninger and A. B. Schwartz, *Lancet*, 2013, **381**, 557–564.
30 L. R. Hochberg, M. D. Serruya, G. M. Friehs, J. A. Mukand, M. Saleh, A. H. Caplan, A. Branner, D. Chen, R. D. Penn and J. P. Donoghue, *Nature*, 2006, **442**, 164–171.
31 M. D. Gingerich, J. F. Hetke, D. J. Anderson and K. D. Wise, *Transducers' 01 Eurosensors XV*, Springer, 2001, pp. 416–419.
32 M. Kindlundh, P. Norlin and U. G. Hofmann, *Sens. Actuators, B*, 2004, **102**, 51–58.
33 Z. Berces, K. Toth, G. Marton, I. Pal, B. Kovats-Megyesi, Z. Fekete, I. Ulbert and A. Pongracz, *Sci. Rep.*, 2016, **6**, 35944.
34 K. S. Ryu, S. K. Jeong, J. Joo and K. M. Kim, *J. Phys. Chem. B*, 2007, **111**, 731–739.
35 Y. H. Huang and J. B. Goodenough, *Chem. Mater.*, 2008, **20**, 7237–7241.
36 W. Xiao, J. S. Chen, Q. Lu and X. W. Lou, *J. Phys. Chem. C*, 2010, **114**, 12048–12051.
37 A. Altuna, L. Menendez de la Prida, E. Bellistri, G. Gabriel, A. Guimera, J. Berganzo, R. Villa and L. J. Fernandez, *Biosens. Bioelectron.*, 2012, **37**, 1–5.
38 E. M. Thaning, M. L. Asplund, T. A. Nyberg, O. W. Inganas and H. von Holst, *J. Biomed. Mater. Res., Part B*, 2010, **93**, 407–415.

39 S. Nimbalkar, E. Castagnola, A. Balasubramani, A. Scarpellini, S. Samejima, A. Khorasani, A. Boissenin, S. Thongpang, C. Moritz and S. Kassegne, *Sci. Rep.*, 2018, **8**, 6958.
40 M. Vomero, E. Castagnola, F. Ciarpella, E. Maggiolini, N. Goshi, E. Zucchini, S. Carli, L. Fadiga, S. Kassegne and D. Ricci, *Sci. Rep.*, 2017, **7**, 40332.
41 A. G. Zestos, C. B. Jacobs, E. Trikantzopoulos, A. E. Ross and B. J. Venton, *Anal. Chem.*, 2014, **86**, 8568–8575.
42 F. Vitale, S. R. Summerson, B. Aazhang, C. Kemere and M. Pasquali, *ACS Nano*, 2015, **9**, 4465–4474.
43 E. W. Keefer, B. R. Botterman, M. I. Romero, A. F. Rossi and G. W. Gross, *Nat. Nanotechnol.*, 2008, **3**, 434–439.
44 G. Gao, T. Cagin and W. A. Goddard III, *Nanotechnology*, 1998, **9**, 184.
45 V. Lovat, D. Pantarotto, L. Lagostena, B. Cacciari, M. Grandolfo, M. Righi, G. Spalluto, M. Prato and L. Ballerini, *Nano Lett.*, 2005, **5**, 1107–1110.
46 A. H. Nayak and T. R. Makam, *ACS Nano*, 2011, **5**, 4670–4678.
47 S. Stankovich, D. A. Dikin, G. H. Dommett, K. M. Kohlhaas, E. J. Zimney, E. A. Stach, R. D. Piner, S. T. Nguyen and R. S. Ruoff, *Nature*, 2006, **442**, 282–286.
48 H. Y. Mao, S. Laurent, W. Chen, O. Akhavan, M. Imani, A. A. Ashkarran and M. Mahmoudi, *Chem. Rev.*, 2013, **113**, 3407–3424.
49 Y. Zhang, S. F. Ali, E. Dervishi, Y. Xu, Z. Li, D. Casciano and A. S. Biris, *ACS Nano*, 2010, **4**, 3181–3186.
50 Y. R. Kim, S. Bong, Y. J. Kang, Y. Yang, R. K. Mahajan, J. S. Kim and H. Kim, *Biosens. Bioelectron.*, 2010, **25**, 2366–2369.
51 A. M. Díez-Pascual, *Int. J. Mol. Sci.*, 2020, **21**, 3563.
52 J. Maughan, P. J. Gouveia, J. G. Gonzalez, L. M. Leahy, I. Woods, C. O'Connor, T. McGuire, J. R. Garcia, D. G. O. Shea, S. F. McComish, O. D. Kennedy, M. A. Caldwell, A. Dervan, J. N. Coleman and F. J. O'Brien, *Appl. Mater. Today*, 2022, **29**, 101629.
53 A. Altuna, E. Bellistri, E. Cid, P. Aivar, B. Gal, J. Berganzo, G. Gabriel, A. Guimera, R. Villa, L. J. Fernandez and L. Menendez de la Prida, *Lab Chip*, 2013, **13**, 1422–1430.
54 G. Dijk, A. Kaszas, J. Pas and R. P. O'Connor, *Microsyst. Nanoeng.*, 2022, **8**, 90.
55 J. T. Kuo, B. J. Kim, S. A. Hara, C. D. Lee, C. A. Gutierrez, T. Q. Hoang and E. Meng, *Lab Chip*, 2013, **13**, 554–561.
56 K. Wang, C. L. Frewin, D. Esrafilzadeh, C. Yu, C. Wang, J. J. Pancrazio, M. Romero-Ortega, R. Jalili and G. Wallace, *Adv. Mater.*, 2019, **31**, e1805867.
57 Y. Lu, H. Lyu, A. G. Richardson, T. H. Lucas and D. Kuzum, *Sci. Rep.*, 2016, **6**, 33526.
58 X. Tang, H. Shen, S. Zhao, N. Li and J. Liu, *Nat. Electron.*, 2023, **6**, 109–118.
59 L. Luan, X. Wei, Z. Zhao, J. J. Siegel, O. Potnis, C. A. Tuppen, S. Lin, S. Kazmi, R. A. Fowler, S. Holloway, A. K. Dunn, R. A. Chitwood and C. Xie, *Sci. Adv.*, 2017, **3**, e1601966.
60 J. A. Rogers, T. Someya and Y. Huang, *Science*, 2010, **327**, 1603–1607.
61 E. J. Welle, J. E. Woods, A. A. Jiman, J. M. Richie, E. C. Bottorff, Z. Ouyang, J. P. Seymour, P. R. Patel, T. M. Bruns and C. A. Chestek, *IEEE Trans. Neural Syst. Rehabil. Eng.*, 2021, **29**, 993–1003.
62 T. L. Li, Y. Liu, C. Forro, X. Yang, L. Beker, Z. Bao, B. Cui and S. P. Pasca, *Biomaterials*, 2022, **290**, 121825.
63 X. Wang, M. Wang, H. Sheng, L. Zhu, J. Zhu, H. Zhang, Y. Liu, L. Zhan, X. Wang, J. Zhang, X. Wu, Z. Suo, W. Xi and H. Wang, *Biomaterials*, 2022, **281**, 121352.
64 L. Gao, J. Wang, Y. Zhao, H. Li, M. Liu, J. Ding, H. Tian, S. Guan and Y. Fang, *Adv. Mater.*, 2022, **34**, 2107343.
65 K. J. Seo, M. Hill, J. Ryu, C.-H. Chiang, I. Rachinskiy, Y. Qiang, D. Jang, M. Trumpis, C. Wang, J. Viventi and H. Fang, *npj Flexible Electron.*, 2023, **7**, 40.
66 Mc Lo, S. Wang, S. Singh, V. B. Damodaran, H. M. Kaplan, J. Kohn, D. I. Shreiber and J. D. Zahn, *Biomed. Microdevices*, 2015, **17**, 34.
67 D. Kil, M. Bovet Carmona, F. Ceyssens, M. Deprez, L. Brancato, B. Nuttin, D. Balschun and R. Puers, *Micromachines*, 2019, **10**, 61.
68 J. Agorelius, F. Tsanakalis, A. Friberg, P. T. Thorbergsson, L. M. E. Pettersson and J. Schouenborg, *Front. Neurosci.*, 2015, **9**, 331.
69 N. Sharafkhani, J. M. Long, S. D. Adams and A. Z. Kouzani, *Sens. Actuators, A*, 2023, **363**, 114759.
70 F. Ceyssens, M. Deprez, N. Turner, D. Kil, K. van Kuyck, M. Welkenhuysen, B. Nuttin, S. Badylak and R. Puers, *J. Neural Eng.*, 2017, **14**, 014001.
71 C. M. Tringides, N. Vachicouras, I. de Lazaro, H. Wang, A. Trouillet, B. R. Seo, A. Elosegui-Artola, F. Fallegger, Y. Shin, C. Casiraghi, K. Kostarelos, S. P. Lacour and D. J. Mooney, *Nat. Nanotechnol.*, 2021, **16**, 1019–1029.
72 A. Canales, S. Park, A. Kilias and P. Anikeeva, *Acc. Chem. Res.*, 2018, **51**, 829–838.
73 T. I. Kim, J. G. McCall, Y. H. Jung, X. Huang, E. R. Siuda, Y. Li, J. Song, Y. M. Song, H. A. Pao, R. H. Kim, C. Lu, S. D. Lee, I. S. Song, G. Shin, R. Al-Hasani, S. Kim, M. P. Tan, Y. Huang, F. G. Omenetto, J. A. Rogers and M. R. Bruchas, *Science*, 2013, **340**, 211–216.
74 F. Wu, E. Stark, P. C. Ku, K. D. Wise, G. Buzsaki and E. Yoon, *Neuron*, 2015, **88**, 1136–1148.
75 H. Shin, S. Jeong, J. H. Lee, W. Sun, N. Choi and I. J. Cho, *Nat. Commun.*, 2021, **12**, 492.
76 H. Yuk, B. Lu and X. Zhao, *Chem. Soc. Rev.*, 2019, **48**, 1642–1667.
77 S. P. Lacour, G. Courtine and J. Guck, *Nat. Rev. Mater.*, 2016, **1**, 16063.
78 P. Fattahi, G. Yang, G. Kim and M. R. Abidian, *Adv. Mater.*, 2014, **26**, 1846–1885.
79 C. Hassler, T. Boretius and T. Stieglitz, *J. Polym. Sci., Part B: Polym. Phys.*, 2011, **49**, 18–33.
80 J. W. Salatino, K. A. Ludwig, T. D. Y. Kozai and E. K. Purcell, *Nat. Biomed. Eng.*, 2017, **1**, 862–877.
81 J. Rivnay, H. Wang, L. Fenno, K. Deisseroth and G. G. Malliaras, *Sci. Adv.*, 2017, **3**, e1601649.

82 T. D. Y. Kozai, K. Catt, X. Li, Z. V. Gugel, V. T. Olafsson, A. L. Vazquez and X. T. Cui, *Biomaterials*, 2015, **37**, 25–39.
83 T. D. Kozai, A. S. Jaquins-Gerstl, A. L. Vazquez, A. C. Michael and X. T. Cui, *ACS Chem. Neurosci.*, 2015, **6**, 48–67.
84 V. S. Polikov, P. A. Tresco and W. M. Reichert, *J. Neurosci. Methods*, 2005, **148**, 1–18.
85 Y. T. Kim, R. W. Hitchcock, M. J. Bridge and P. A. Tresco, *Biomaterials*, 2004, **25**, 2229–2237.
86 D. H. Szarowski, M. D. Andersen, S. Retterer, A. J. Spence, M. Isaacson, H. G. Craighead, J. N. Turner and W. Shain, *Brain Res.*, 2003, **983**, 23–35.
87 M. L. Block and J. S. Hong, *Prog. Neurobiol.*, 2005, **76**, 77–98.
88 M. L. Block, L. Zecca and J. S. Hong, *Nat. Rev. Neurosci.*, 2007, **8**, 57–69.
89 S. W. Turner and J. N. Szarowski, *Exp. Neurol.*, 1999, **156**, 33–49.
90 M. Gulino, D. Kim, S. Pane, S. D. Santos and A. P. Pego, *Front. Neurosci.*, 2019, **13**, 689.
91 T. D. Kozai, J. R. Eles, A. L. Vazquez and X. T. Cui, *J. Neurosci. Methods*, 2016, **258**, 46–55.
92 L. W. Tien, F. Wu, M. D. Tang-Schomer, E. Yoon, F. G. Omenetto and D. L. Kaplan, *Adv. Funct. Mater.*, 2013, **23**, 3185–3193.
93 G. A. McCallum, X. Sui, C. Qiu, J. Marmerstein, Y. Zheng, T. E. Eggers, C. Hu, L. Dai and D. M. Durand, *Sci. Rep.*, 2017, **7**, 11723.
94 D. Khodagholy, J. N. Gelinas, T. Thesen, W. Doyle, O. Devinsky, G. G. Malliaras and G. Buzsaki, *Nat. Neurosci.*, 2015, **18**, 310–315.
95 W. Lee, S. Kobayashi, M. Nagase, Y. Jimbo, I. Saito, Y. Inoue, T. Yambe, M. Sekino, G. G. Malliaras, T. Yokota, M. Tanaka and T. Someya, *Sci. Adv.*, 2018, **4**, eaau2426.
96 J. Liu, T. M. Fu, Z. Cheng, G. Hong, T. Zhou, L. Jin, M. Duvvuri, Z. Jiang, P. Kruskal, C. Xie, Z. Suo, Y. Fang and C. M. Lieber, *Nat. Nanotechnol.*, 2015, **10**, 629–636.
97 Z. Yan, M. Han, Y. Shi, A. Badea, Y. Yang, A. Kulkarni, E. Hanson, M. E. Kandel, X. Wen, F. Zhang, Y. Luo, Q. Lin, H. Zhang, X. Guo, Y. Huang, K. Nan, S. Jia, A. W. Oraham, M. B. Mevis, J. Lim, X. Guo, M. Gao, W. Ryu, K. J. Yu, B. G. Nicolau, A. Petronico, S. S. Rubakhin, J. Lou, P. M. Ajayan, K. Thornton, G. Popescu, D. Fang, J. V. Sweedler, P. V. Braun, H. Zhang, R. G. Nuzzo, Y. Huang, Y. Zhang and J. A. Rogers, *Proc. Natl. Acad. Sci. U. S. A.*, 2017, **114**, E9455–E9464.
98 J. M. Lee, D. Lin, G. Hong, K.-H. Kim, H.-G. Park and C. M. Lieber, *Nano Lett.*, 2022, **22**, 4552–4559.
99 J. P. Seymour and D. R. Kipke, *Biomaterials*, 2007, **28**, 3594–3607.
100 G. C. McConnell, T. M. Schneider, D. J. Owens and R. V. Bellamkonda, *IEEE Trans. Biomed. Eng.*, 2007, **54**, 1097–1107.
101 Y. Zhou, C. Gu, J. Liang, B. Zhang, H. Yang, Z. Zhou, M. Li, L. Sun, T. H. Tao and X. Wei, *Microsyst. Nanoeng.*, 2022, **8**, 118.
102 J. R. Eles, A. L. Vazquez, T. D. Y. Kozai and X. T. Cui, *Biomaterials*, 2018, **174**, 79–94.
103 M. D. Ferro and N. A. Melosh, *Adv. Funct. Mater.*, 2018, **28**, 1704335.
104 T. Chung, J. Q. Wang, J. Wang, B. Cao, Y. Li and S. W. Pang, *J. Neural Eng.*, 2015, **12**, 056018.
105 J. B. Johnson, *Phys. Rev.*, 1927, **32**, 97.
106 T. D. Kozai and A. L. Vazquez, *J. Mater. Chem. B*, 2015, **3**, 4965–4978.
107 O. Veiseh, J. C. Doloff, M. Ma, A. J. Vegas, H. H. Tam, A. R. Bader, J. Li, E. Langan, J. Wyckoff, W. S. Loo, S. Jhunjhunwala, A. Chiu, S. Siebert, K. Tang, J. Hollister-Lock, S. Aresta-Dasilva, M. Bochenek, J. Mendoza-Elias, Y. Wang, M. Qi, D. M. Lavin, M. Chen, N. Dholakia, R. Thakrar, I. Lacik, G. C. Weir, J. Oberholzer, D. L. Greiner, R. Langer and D. G. Anderson, *Nat. Mater.*, 2015, **14**, 643–651.
108 C. Liu, Y. Zhao, X. Cai, Y. Xie, T. Wang, D. Cheng, L. Li, R. Li, Y. Deng, H. Ding, G. Lv, G. Zhao, L. Liu, G. Zou, M. Feng, Q. Sun, L. Yin and X. Sheng, *Microsyst. Nanoeng.*, 2020, **6**, 64.
109 Q. Liang, Z. Shen, X. Sun, D. Yu, K. Liu, S. M. Mugo, W. Chen, D. Wang and Q. Zhang, *Adv. Mater.*, 2023, **35**, e2211159.
110 J. Nam, H. K. Lim, N. H. Kim, J. K. Park, E. S. Kang, Y. T. Kim, C. Heo, O. S. Lee, S. G. Kim, W. S. Yun, M. Suh and Y. H. Kim, *ACS Nano*, 2020, **14**, 664–675.
111 J. Zhang, L. Wang, Y. Xue, I. M. Lei, X. Chen, P. Zhang, C. Cai, X. Liang, Y. Lu and J. Liu, *Adv. Mater.*, 2022, **35**, e2209324.
112 S. Middya, A. Carnicer-Lombarte, V. F. Curto, S. Hilton, A. Genewsky, A. L. Rutz, D. G. Barone, G. S. Kaminski Schierle, A. Sirota and G. G. Malliaras, *Adv. Electron. Mater.*, 2023, **9**, 2200883.
113 S. Sassolini, H. Adesnik, S. Dhuey, R. Lambert, P. Micheletti, G. Telian, A. Koshelev, M. West and V. Lanzio, *J. Micro/Nanolithogr., MEMS, MOEMS*, 2018, **17**, 025503.
114 D. Qi, Z. Liu, Y. Liu, Y. Jiang, W. R. Leow, M. Pal, S. Pan, H. Yang, Y. Wang, X. Zhang, J. Yu, B. Li, Z. Yu, W. Wang and X. Chen, *Adv. Mater.*, 2017, **29**, 1702800.
115 C. H. Chiang, S. M. Won, A. L. Orsborn, K. J. Yu, M. Trumpis, B. Bent, C. Wang, Y. Xue, S. Min, V. Woods, C. Yu, B. Kim, S. Kim, R. Huq, J. Li, K. Seo, F. Vitale, A. Richardson, H. Fang, Y. Huang, K. Shepard, B. Pesaran, J. Rogers and J. Viventi, *Sci. Transl. Med.*, 2020, **538**, eaay4682.
116 S. Guan, J. Wang, X. Gu, Y. Zhao, R. Hou, H. Fan, L. Zou, L. Gao, M. Du, C. Li and Y. Fang, *Sci. Adv.*, 2019, **3**, eaav2842.
117 M. Elon, *J. Med. Internet Res.*, 2019, **21**, e16194.
118 J. J. Jun, N. A. Steinmetz, J. H. Siegle, D. J. Denman, M. Bauza, B. Barbarits, A. K. Lee, C. A. Anastassiou, A. Andrei, Ç. Aydın, M. Barbic, T. J. Blanche, V. Bonin, J. Couto, B. Dutta, S. L. Gratiy, D. A. Gutnisky, M. Häusser, B. Karsh, P. Ledochowitsch, C. M. Lopez, C. Mitelut,

S. Musa, M. Okun, M. Pachitariu, J. Putzeys, P. D. Rich, C. Rossant, W.-L. Sun, K. Svoboda, M. Carandini, K. D. Harris, C. Koch, J. O'Keefe and T. D. Harris, *Nature*, 2017, **551**, 232–236.

119 M. Vomero, F. Ciarpella, E. Zucchini, M. Kirsch, L. Fadiga, T. Stieglitz and M. Asplund, *Biomaterials*, 2022, **281**, 121372.

120 E. T. Zhao, J. M. Hull, N. Mintz Hemed, H. Uluşan, J. Bartram, A. Zhang, P. Wang, A. Pham, S. Ronchi, J. R. Huguenard, A. Hierlemann and N. A. Melosh, *Sci. Adv.*, 2023, **9**, eadf9524.

121 K. Sahasrabuddhe, A. A. Khan, A. P. Singh, T. M. Stern, Y. Ng, A. Tadić, P. Orel, C. LaReau, D. Pouzzner, K. Nishimura, K. M. Boergens, S. Shivakumar, M. S. Hopper, B. Kerr, M. E. S. Hanna, R. J. Edgington, I. McNamara, D. Fell, P. Gao, A. Babaie-Fishani, S. Veijalainen, A. V. Klekachev, A. M. Stuckey, B. Luyssaert, T. D. Y. Kozai, C. Xie, V. Gilja, B. Dierickx, Y. Kong, M. Straka, H. S. Sohal and M. R. Angle, *J. Neural Eng.*, 2020, **18**, 015002.

122 L. A. Camuñas-Mesa and R. Q. Quiroga, *Neural Comput.*, 2013, **25**, 1191–1212.

123 C. A. R. Chapman, L. Wang, H. Chen, J. Garrison, P. J. Lein and E. Seker, *Adv. Funct. Mater.*, 2017, **27**, 1604631.

124 H. Woo, S. Kim, H. Nam, W. Choi, K. Shin, K. Kim, S. Yoon, G. H. Kim, J. Kim and G. Lim, *Anal. Chem.*, 2021, **93**, 11765–11774.

125 G. H. Kim, K. Kim, H. Nam, K. Shin, W. Choi, J. H. Shin and G. Lim, *Sens. Actuators, B*, 2017, **252**, 152–158.

126 N. A. Kotov, J. O. Winter, I. P. Clements, E. Jan, B. P. Timko, S. Campidelli, S. Pathak, A. Mazzatenta, C. M. Lieber, M. Prato, R. V. Bellamkonda, G. A. Silva, N. W. S. Kam, F. Patolsky and L. Ballerini, *Adv. Mater.*, 2009, **21**, 3970–4004.

127 D. H. Kim, J. Viventi, J. J. Amsden, J. Xiao, L. Vigeland, Y. S. Kim, J. A. Blanco, B. Panilaitis, E. S. Frechette, D. Contreras, D. L. Kaplan, F. G. Omenetto, Y. Huang, K. C. Hwang, M. R. Zakin, B. Litt and J. A. Rogers, *Nat. Mater.*, 2010, **9**, 511–517.

128 G. Baranauskas, E. Maggiolini, E. Castagnola, A. Ansaldo, A. Mazzoni, G. N. Angotzi, A. Vato, D. Ricci, S. Panzeri and L. Fadiga, *J. Neural Eng.*, 2011, **8**, 066013.

129 C. H. Chen, C. T. Lin, W. L. Hsu, Y. C. Chang, S. R. Yeh, L. J. Li and D. J. Yao, *Nanomedicine*, 2013, **9**, 600–604.

130 R. J. Vetter, J. C. Williams, J. F. Hetke, E. A. Nunamaker and D. R. Kipke, *IEEE Trans. Biomed. Eng.*, 2004, **51**, 896–904.

131 H. Fishman, K. Wang, H. Dai and J. S. Harris, *Nano Lett.*, 2006, **6**, 2043–2048.

132 S. F. Cogan, T. D. Plante and J. Ehrlich, *Proc. IEEE Conf. Eng. Med. Biol. Soc.*, 2004, vol. 2004, pp. 4153–4156.

133 Y. Lu, T. Wang, Z. Cai, Y. Cao, H. Yang and Y. Y. Duan, *Sens. Actuators, B*, 2009, **137**, 334–339.

134 D. Martin, Y. Xiao, X. Cui and M. Shenai, *Appl. Biochem. Biotechnol.*, 2006, **128**, 117–130.

135 K. A. Ludwig, N. B. Langhals, M. D. Joseph, S. M. Richardson-Burns, J. L. Hendricks and D. R. Kipke, *J. Neural Eng.*, 2011, **8**, 014001.

136 S. Venkatraman, J. Hendricks, Z. A. King, A. J. Sereno, S. Richardson-Burns, D. Martin and J. M. Carmena, *IEEE Trans. Neural Syst. Rehabil. Eng.*, 2011, **19**, 307–316.

137 V. Lee, X. Cui and Y. Raphael, *J. Biomed. Mater. Res.*, 2001, **56**, 261–272.

138 X. Liu, Z. Yue, M. J. Higgins and G. G. Wallace, *Biomaterials*, 2011, **32**, 7309–7317.

139 M. Lee, H. J. Shim, C. Choi and D.-H. Kim, *Nano Lett.*, 2019, **19**, 2741–2749.

140 X. Shi, Y. Xiao, H. Xiao, G. Harris, T. Wang and J. Che, *Colloids Surf., B*, 2016, **145**, 768–776.

141 H. Woo, S. Kim, H. Nam, W. Choi, K. Shin, K. Kim, S. Yoon, G. H. Kim, J. Kim and G. Lim, *Anal. Chem.*, 2021, **93**, 11765–11774.

142 A. Hess-Dunning and D. Tyler, *Micromachines*, 2018, **9**, 583.

143 S. Liu, Y. Wang, Y. Zhao, L. Liu, S. Sun, S. Zhang, H. Liu, S. Liu, Y. Li, F. Yang, M. Jiao, X. Sun, Y. Zhang, R. Liu, X. Mu, H. Wang, S. Zhang, J. Yang, X. Xie, X. Duan, J. Zhang, G. Hong, X. D. Zhang and D. Ming, *Adv. Mater.*, 2023, **36**, e2304297.

144 L. C. Wang, M. H. Wang, C. F. Ge, B. W. Ji, Z. J. Guo, X. L. Wang, B. Yang, C. Y. Li and J. Q. Liu, *Biosens. Bioelectron.*, 2019, **145**, 111661.

145 P. J. Rousche, D. S. Pellinen, D. P. Pivin, J. C. Williams, R. J. Vetter and D. R. Kipke, *IEEE Trans. Biomed. Eng.*, 2001, **48**, 361–371.

146 K. C. Cheung, P. Renaud, H. Tanila and K. Djupsund, *Biosens. Bioelectron.*, 2007, **22**, 1783–1790.

147 N. V. Apollo, M. I. Maturana, W. Tong, D. A. X. Nayagam, M. N. Shivdasani, J. Foroughi, G. G. Wallace, S. Prawer, M. R. Ibbotson and D. J. Garrett, *Adv. Funct. Mater.*, 2015, **25**, 3551–3559.

148 C. Xie, J. Liu, T. M. Fu, X. Dai, W. Zhou and C. M. Lieber, *Nat. Mater.*, 2015, **14**, 1286–1292.

149 X. Wei, L. Luan, Z. Zhao, X. Li, H. Zhu, O. Potnis and C. Xie, *Adv. Sci.*, 2018, **5**, 1700625.

150 J. Wang, Q. Zhao, Y. Wang, Q. Zeng, T. Wu and X. Du, *Adv. Mater. Technol.*, 2019, **4**, 1900566.

151 L. Gao, S. Lv, Y. Shang, S. Guan, H. Tian, Y. Fang, J. Wang and H. Li, *Nano Lett.*, 2023, **24**, 829–835.

152 X. Strakosas, H. Biesmans, T. Abrahamsson, K. Hellman, M. S. Ejneby, M. J. Donahue, P. Ek, F. Ekström, M. Savvakis, M. Hjort, D. Bliman, M. Linares, C. Lindholm, E. Stavrinidou, J. Y. Gerasimov, D. T. Simon, R. Olsson and M. Berggren, *Science*, 2023, **379**, 795–802.

153 X. Yang, T. Zhou, T. J. Zwang, G. Hong, Y. Zhao, R. D. Viveros, T. M. Fu, T. Gao and C. M. Lieber, *Nat. Mater.*, 2019, **18**, 510–517.

154 G. M. Bahareh, J. Taraneh, S. Fatemeh, J. W. Kevin, M. Richard and S. Mohamad, *Mater. Sci. Eng.*, 2016, **68**, 642–650.

155 D. O. Adewole, L. A. Struzyna, J. C. Burrell, J. P. Harris, A. D. Nemes, D. Petrov, R. H. Kraft, H. I. Chen, M. D. Serruya, J. A. Wolf and D. K. Cullen, *Sci. Adv.*, 2021, **7**, eaay5347.

156 Y. Lee, C. Kong, J. W. Chang and S. B. Jun, *J. Korean Med. Sci.*, 2019, **34**, e24.

157 K. C. Spencer, J. C. Sy, K. B. Ramadi, A. M. Graybiel, R. Langer and M. J. Cima, *Sci. Rep.*, 2017, **7**, 1952.
158 J. L. Skousen, M. J. Bridge and P. A. Tresco, *Biomaterials*, 2015, **36**, 33–43.
159 C. Chen, X. Kong and I. S. Lee, *Biomed. Mater.*, 2015, **11**, 014108.
160 M. Leber, R. Bhandari, F. Solzbacher and S. Negi, *2017 19th International Conference on Solid-State Sensors, Actuators and Microsystems*, 2017, pp. 1726–1729.
161 W. He and R. V. Bellamkonda, *Biomaterials*, 2005, **26**, 2983–2990.
162 Z. R. Wu, J. Ma, B. F. Liu, Q. Y. Xu and F. Z. Cui, *J. Biomed. Mater. Res.*, 2007, **81**, 355–362.
163 Y. H. Kim, N. S. Baek, Y. H. Han, M. A. Chung and S. D. Jung, *J. Neurosci. Methods*, 2011, **202**, 38–44.
164 C. Boehler, D. M. Vieira, U. Egert and M. Asplund, *ACS Appl. Mater. Interfaces*, 2020, **12**, 14855–14865.
165 C. A. R. Chapman, L. Wang, H. Chen, J. Garrison, P. J. Lein and E. Seker, *Adv. Funct. Mater.*, 2017, **27**, 1604631.
166 J. Lee, M. Pyo, S. H. Lee, J. Kim, M. Ra, W. Y. Kim, B. J. Park, C. W. Lee and J. M. Kim, *Nat. Commun.*, 2014, **5**, 3736.
167 B. Ji, C. Ge, Z. Guo, L. Wang, M. Wang, Z. Xie, Y. Xu, H. Li, B. Yang, X. Wang, C. Li and J. Liu, *Biosens. Bioelectron.*, 2020, **153**, 112009.
168 A. Vazquez-Guardado, Y. Yang, A. J. Bandodkar and J. A. Rogers, *Nat. Neurosci.*, 2020, **23**, 1522–1536.
169 S. Park, Y. Guo, X. Jia, H. K. Choe, B. Grena, J. Kang, J. Park, C. Lu, A. Canales, R. Chen, Y. S. Yim, G. B. Choi, Y. Fink and P. Anikeeva, *Nat. Neurosci.*, 2017, **20**, 612–619.
170 D. J. Poxson, E. O. Gabrielsson, A. Bonisoli, U. Linderhed, T. Abrahamsson, I. Matthiesen, K. Tybrandt, M. Berggren and D. T. Simon, *ACS Appl. Mater. Interfaces*, 2019, **11**, 14200–14207.
171 M. Seitanidou, R. Blomgran, G. Pushpamithran, M. Berggren and D. T. Simon, *Adv. Healthcare Mater.*, 2019, **8**, e1900813.